Transactions, SMiRT-24
BEXCO, Busan, Korea - August 20-25, 2017
Division III

AIRCRAFT IMPACT INDUCED VIBRATIONS ON BURIED STRUCTURES

Dr. Manya Deyanova [1], Anton Andonov [2], Dr. Ming Tan [3], James Marsden [4]

[1] Structural Engineer, Mott Macdonald Ltd, Bulgaria
[2] Principal Engineer, Mott Macdonald Ltd, Bulgaria
[3] Discipline Lead for Advanced Analysis, Mott MacDonald Ltd, United Kingdom
[4] Civil Engineer, Design Authority, Nuclear New Build, EDF Energy, UK

ABSTRACT

Buried structures are often considered resistant to impact loads due to the natural barrier of the soil medium surrounding them. In case of aircraft impact, the safety of the buried structures is usually justified by screening based on the physical separation, i.e. distance from the source. The depth and distance from the impact zone at which the soil barrier will be effective depend on the intensity of the induced vibrations, the soil type and the vulnerability of the structure and its equipment. The evaluation of the expected demand and the present capacity requires careful consideration of several important aspects: how to represent the impact energy, how the stress wave propagates and attenuates with distance, what parameters best describe the damage potential of the induced vibrations and how to relate different structural damage states to these parameters.

The paper studies the application of various methods to assess the damage to a buried reinforced concrete structure due to aircraft impact induced vibrations at various distances and depths from the source. Four different types of aircraft – large, medium, small commercial and military aircraft, were considered. The results are discussed and are summarised in damage-distance matrices, associated with confidence levels, which weigh the assumptions and the uncertainties of the applied analysis methods.

INTRODUCTION

One way to protect a structure from aircraft impact (AI) or blast load is to bury it and to take advantage of the energy dissipation as work is done by the propagating shock wave in plastically deforming the soil matrix. To find the depth and the distance from the impact zone at which this barrier would be effective and to assess the damage to the structure and its equipment is of critical importance, especially in the nuclear power sector.

While guidelines for the evaluation of the damage potential of blast groundshocks could be found in the technical literature (HA SEDD NAWCCC DRD, 2001; Smith and Hetherington, 1994), for AI induced vibrations there is no ready-to-use routine and different methods have to be adapted to solve such a problem. Key aspects are: 1) the evaluation of the capacity of the underground structure with the associated likely global and local failure mechanism, with due attention to brittle failure of sections; 2) the selection of adequate parameters to quantify the magnitude of transient disturbance; 3) consideration for soil-structure interaction (SSI) phenomenon, whether directly accounted for or through assumptions for reflected overpressure onto the structure; 4) practical form of comparing demand and capacity and 5) assessment of the uncertainties coupled with the assumptions and approximations towards better interpretation of the final results and efficient decision making.

This paper presents a study on the evaluation of the severity of the damage to an underground reinforced concrete (RC) structure due to a possible AI on the site platform. Different methods for the evaluation of the intensity of the induced vibrations and the capacity of the structure were implemented and the results compared. All of the aspects listed above were carefully considered and reasonable assumptions

were made. The conclusions were presented in terms of damage-distance matrices which predict with certain level of confidence the expected damage to the underground structure at different depths and distances away from the impact zone. Based on them, zones with certain structural failure and zones with no damage could be easily distinguished.

PROBLEM DESCRIPTION

Different cases were considered in the study. Two soil types in three configurations were adopted: loose sand, Soil Type 1, (Layer 1) and dense sand, Soil Type 2, (Layer 2), either in a uniformed soil medium with each of the soil types or in a layered soil medium. This is shown in Figure 1. The shear wave velocities V_s, the friction angles and the specific weights of the soil types were assumed accordingly and the other necessary mechanical parameters were derived from them. The attenuation coefficient n was selected based on TM 5-855-1 (Smith and Hetherington, 1994). The impact load corresponded to four types of aircraft: Large, Medium and Small Commercial and Military aircraft. The adopted load functions for each of them are shown in Figure 1. It was assumed that the aircraft hits the horizontal surface at 30º and at two possible impact depths d_s=1m and d_s=2m. The mass, the impact velocity and the dimensions of the footprint of each aircraft were also know at the start.

The groundshock intensity was evaluated at several pre-set points of interest (the blue dots in Figure 1) at six different horizontal distances li away from the impact zone and four different depths d_t. The buried structure is a RC square tunnel with known material properties and reinforcement detailing. The aspect ratio of the walls is h/l_{cl}=3. Since all the analyses were performed in two-dimensional (2D) space, only a 1m-long section of the tunnel was considered

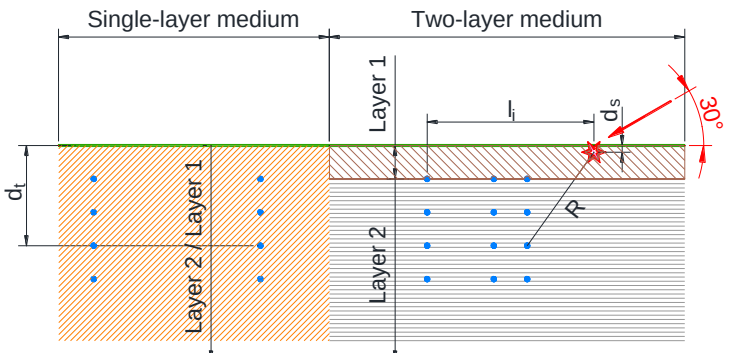

Layer 1 – Loose, dry poorly graded sand, Vs=200m/s – n=3.25 [2]
Layer 2 – Dense sand with high relative density, Vs=500m/s – n=2.5 [2]

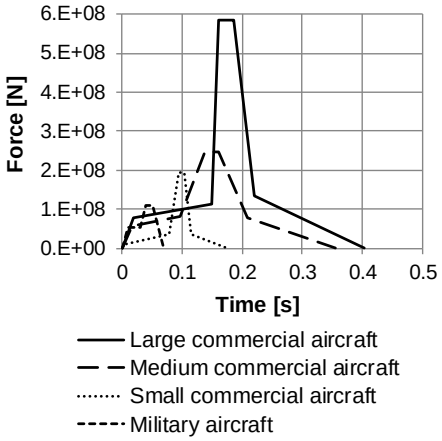

Figure 1 Soil types, soil layers and load functions of the types of aircraft considered in the analyses

METHODOLOGY

The methodology of the study is illustrated with the flow chart in Figure 2. The capacity of the structure was evaluated based on probable global and local failure modes with due consideration for brittle failure of sections. The intensity of the induced vibrations was obtained with four different methods: Method 1, which implements analytical methodology for blast wave soil propagation by representing the impact with an equivalent point TNT explosion; Method 2, in which the AI was represented by sin-wave vibrations induced in an equivalent elastic soil column; Method 3, which makes use of dynamic analysis of finite element (FE) linear elastic 2D models; Method 4, which implements the same FE model but this time the structure is added and the SSI is directly accounted for by means of contact elements. The first three methods are free-field analysis, where the intensity parameters were found in the points of interest in the soil medium and

then assumptions were made for the expected reflected overpressure onto the structure based on recommendations by Smith and Hetherington (1994):

$$p_{0,structure} = 1.25 \cdot p_{0,free\text{-}field} \rightarrow \text{pressure} \qquad v_{structure} = 2 \cdot PPV_{free\text{-}field} \rightarrow \text{velocity}$$

$$\Delta_{structure,\ relative} = \Delta_{free\text{-}field} \rightarrow \text{displacement}$$

Method 4, however, accounted for the interaction between the structure and the soil and allowed for the direct recording of the internal forces of the elements of the tunnel.

The structural capacity was compared to the demand in terms of pressure-impulse diagrams, drift limits and possible brittle local failure. The assumptions and uncertainties of the first three methods were weighed and the results were assigned certain confidence levels. As a result, damage-distance matrices were obtained which predict structural damage expected at different distances away from the impact area and how confident this prediction is within the limitations of the present study. The results from Method 4 helped to increase the confidence of the predictions at distances close to the impact zone.

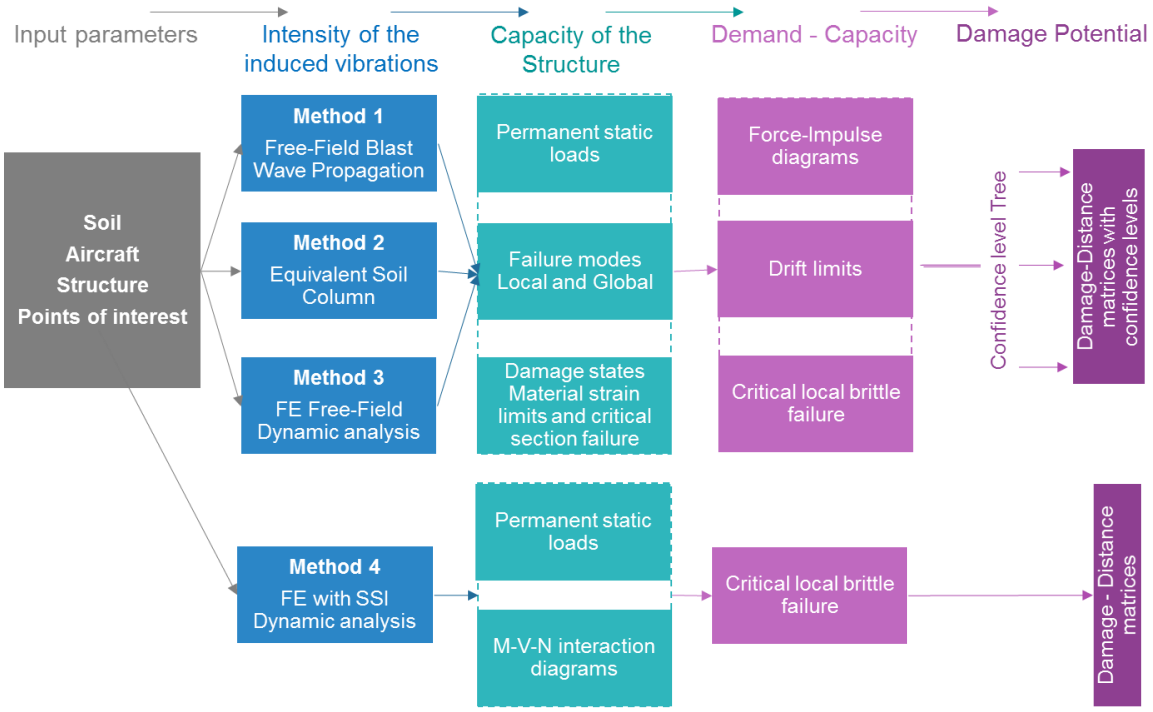

Figure 2 Methodology of the study

INTENSITY OF THE INDUCED VIBRATIONS - DEMAND

Method 1 - Free-field blast wave propagation in soil

In Method 1 the aircraft impact was represented by a blast point load with an equivalent TNT mass and the attenuation of the impact wave was calculated using analytical methods for blasts by Smith and Hetherington (1994). Three different soil medium were analysed (Figure 1): uniform soil with properties for Layer 1; uniform soil with properties for Layer 2 and layered soil medium. The impact was assumed at two different depths: d_s=1m and d_s=2m. The impact load was approximated to an isosceles triangle with the bounded area equal to the impact pulse energy $i_0 = M_{AIC}V_0 = Ft_d/2$. The equivalent TNT mass W_{TNT} of explosive was obtained by assuming that $W_{TNT} = ½\ M_{AIC}V_0^2$ / 4184MJ. Peak particle velocity (PPV), peak particle displacement (PPD) and peak pressure p_0 for free-field were obtained using the empirical formulae

(Eq. 1, Eq. 2 and Eq. 3) according to Smith and Hetherington (1994), where the attenuation coefficient n was taken as shown in Figure 1 and the coupling factor f_c was found as a function of the scaled depth of burst $d_s/W_{TNT}^{1/3}$.

$$PPV = 48.8 f_c \left(\frac{2.52R}{W_{TNT}^{1/3}}\right)^{-n} \quad (1) \qquad \frac{PPD}{W_{TNT}^{1/3}} = 60\frac{f_c}{c}\left(\frac{2.52R}{W_{TNT}^{1/3}}\right)^{1-n} \quad (2) \qquad p_0 = \rho PPV\left(c + \frac{n+1}{n-2}PPV\right) \quad (3)$$

A key advantage of this method is that the used empirical attenuation equations were developed precisely for underground blast induced vibrations and are well calibrated. The main drawback is that the impact is represented with a point blast load, the analysis is 2D and SSI is not directly accounted for.

Method 2 - Equivalent soil column, vibrations due to a falling object

In Method 2 the AI was represented by sin-wave vibration induced in an equivalent elastic soil column and the demand of the propagating wave away from the impact zone was obtained by means of attenuation (decay) relationships. Compared to Method 1, in Method 2 the actual impact footprint was considered (engine-to-engine and engine-to-cockpit distances). The section of the vertical soil column, which is directly affected by the impact is assumed to be equal to the horizontal projection of the impact footprint A_{horiz}, when the aircraft hits the ground at an angle with respect to the horizontal axis. Again two impact depths were analysed: d_s=1m and d_s=2m.

The same soil properties were used but this time only for uniform soil media: 1) with the properties for Layer 1; 2) with the properties for Layer 2. The attenuation with distance was based on a formula that combines the geometrical spreading and the material damping. It is presented with Eq. 4, in which ψ=1 (Amick and Gendreau, 2000) for body waves recorded at a given depth and α is the attenuation coefficient according to Dowding (2000). The soil column which is directly affected by the impact load is idealised by a single degree of freedom spring-mass oscillator. According to the conservation of energy, the maximum kinetic energy of the aircraft at the time of impact is equal to the elastic potential energy of the oscillator at its maximum displacement (Eq. 5). The length of the equivalent elastic column was derived by equating the frequency of the impact load to the natural frequency of the soil column (Eq. 6) and the stiffness of the equivalent soil column was calculated based only on the axial stiffness (Eq. 7). The PPV (Eq. 8) was calculated from the equation of motion of a sinusoidal wave, with a frequency equivalent to the assumed impact frequency and particle displacement amplitude equal to x_{max}.

$$V_2 = V_1\left(\frac{R_1}{R_2}\right)^{\psi} e^{-\alpha(R_2-R_1)} \quad (4) \qquad \frac{1}{2}Kx_{max}^2 = \frac{1}{2}M_{AIC}V_0^2 \;\rightarrow\; x_{max} = \sqrt{\frac{M_{AIC}}{K}}V_0 \quad (5)$$

$$f = \frac{1}{t_d} = \frac{V_s}{4L_{col}} \;\rightarrow\; L_{col} = \frac{V_s t_d}{4} \quad (6) \qquad K = \frac{E \cdot A_{horiz.}}{L_{col}} \quad (7)$$

$$PPV = x_{max}\omega = x_{max}2\pi f = x_{max}2\pi\frac{1}{t_d} \quad (8)$$

What Method 2 considered, different from Method 1, is the actual area of the impact load, which directly affects the intensity of the load. The less robust aspects of Method 2, however, are that the assumption for an elastic column and propagation of a sin-wave along it is too crude for such large load intensities like AIs and the method is very sensitive to the attenuation coefficients, which led to a significant difference in the results for the two soil types.

Method 3 - Free-field FE dynamic analysis

In Method 3, the soil medium consisted of two layers (Figure 1) and was modelled with the FE programme LS-DYNA (LSTC, http://www.lstc.com, LSTC, 2014) with elastic shell elements. The stiffness and the damping assigned to these shells were obtained after iteration around the expected strain state of the soil due to the loading. Since the strain rate is different in different zones of the two-dimensional soil medium, each of them was assigned different properties according to the shear modulus degradation and damping rules by Idriss and Sun (1992) for clay (Layer 1) and GEI (1983) for cohesionless soil (Layer 2). Four different models with different soil-medium zonation and crater depths were created. An example for the Large Commercial Aircraft is shown in Figure 3. The initial shear modulus was calculated by considering the effective stress at three depths, for specific void ratios and by using empirical relationships by Zen et al. (1987) for Layer 1 and Kokusho and Esashi (1981) for Layer 2. The size of the FE model was selected to be sufficiently larger than the zone of interest. The size of the elements vary and were optimised to correctly transmit the expected frequency and velocity of the impact wave. Furthermore, non-reflecting boundaries were assigned to the bottom and both sides of the medium in order to best recreate the conditions of a continuum and to eliminate the effect of reflected waves. Additional 1% global viscous damping was assigned to the entire model.

The impact load from each aircraft was modelled with the load functions from Figure 1, distributed on the corresponding footprints. The crater in the vicinity of the impact was with a depth different for each aircraft. The impact load history was assigned to a rigid beam along one of the crater's sides. Implicit time-history analyses were run. As a result, time-history of pressure, force, velocity and displacement in any point or element in the stratum were obtained. Just like in Method 2, in Method 3 the area of the impact load was accounted for, which is one of the reasons for the overall lower demand compared to Method 1 and explains why the smaller aircraft showed larger intensities of the induced vibrations compared to the same from Method 1. What is more, in Method 3 the soil non-linearity is simulated through the equivalent elastic method. Additional iterations for the soil zoning will improve the prediction.

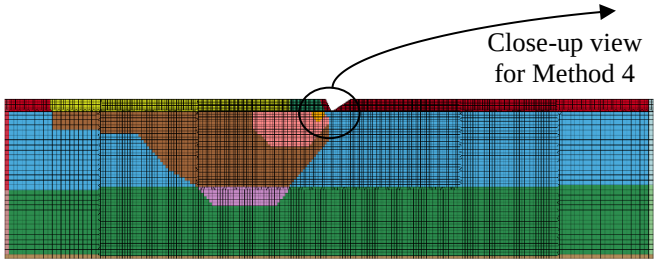

Method 3 Free-field analysis - FE-model mesh. Zones with different mechanical properties of the soil

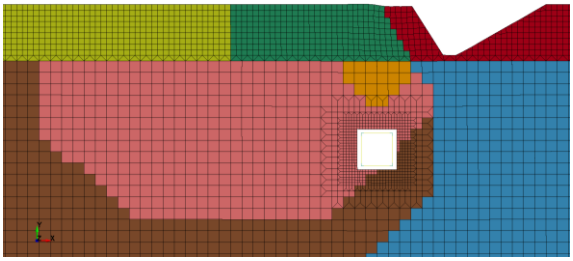

Method 4 SSI - FE-model mesh. Zones with different mechanical properties of the soil medium with the tunnel at l_i and $2d_t$

Figure 3 View of the FE model for the loading with Large Commercial Aircraft

Method 4 - FE non-linear dynamic analysis

The FE models created for Method 4 were based on the models for Method 3. The properties of the soil medium were taken directly from the latter. To the mesh of the soil medium, different for each aircraft type, a 1m-long section of the tunnel was added at different depths and distances according to the investigated cases. The structure was modelled with elastic frame elements and positioned along the mid-axes of the sections. The panel zones were modelled with rigid beams. The redundant soil elements were deleted and those surrounding it were adequately split into smaller elements towards a finer mesh (Figure 3). In addition, null frame elements with negligible stiffness were placed in parallel with the tunnel beams at an offset equal h/2. These null beams, connected to the shells at the inner edges of the stratum opening, were needed to model the contact between the structure and the soil with no penetration and no tension stiffness. The

contact element was type AUTOMATIC GENERAL, according to LS-DYNA, with a friction coefficient 0.4. Implicit dynamic analyses were performed. This time, however, the analyses were run with a smaller calculation step to prevent penetration within the contacts.

The internal forces in each of the four walls of the tunnel were recorded at three different locations: at both ends next to the joints and at mid span. After that, the internal forces from the static analysis with the permanent loads and earth pressure at rest were added, with the corresponding sign, to the recorded time-histories from the dynamic analysis and were compared to the capacity of the section.

The direct modelling of the SSI between the tunnel and the adjacent soil in Method 4 provided most realistic distribution of the internal forces within the structure due to the AI induced vibrations.

CAPACITY OF THE STRUCTURE

The capacity of the structure was estimated considering the continues action of the permanent loads – self-weight, equipment, surcharge load, vertical and horizontal earth pressure at different depths d_t. The superimposed dead load on top of the tunnel from the soil cover was limited to a value of distributed load equal to $\beta\gamma H$, due to the arching effect in the soil above when the gallery settles with respect to the surrounding soil layers. Coefficient β followed recommendations by BD 31/01 (HA SEDD NAWCCC DRD, 2001) for foundations on hard material. The mobilisation of the active and passive horizontal earth pressure was considered, when the induced vibrations try to displace and deform the structure. According to EN 1997 1:2004 very little structural displacements are needed to mobilise fully the active earth pressure. That is why, for the calculation of the structural capacity the active pressure was taken with its full value. However, this is not the case for the passive earth pressure, which, according to the same source, is fully mobilised at displacements between 17.5 to 60 times larger than those for the active earth pressure and the percentage of mobilised passive pressure is not directly proportional to the displacements. This made the process of finding the structural capacity iterative by varying the portion of mobilised passive earth pressure such that the displacements at certain damage states corresponded to it.

Global and localised structural failure mechanisms were investigated. The global force-displacement response was obtained by running a push-over analysis of a frame model in SAP2000. An overview of the model is shown in Error! Reference source not found.. The 1m-segment of the tunnel was modelled with frame elements with a reduced elastic modulus for cracked stiffness $E_{reduced} = E_c\,(EI_{crack}/EI_{gross}) \rightarrow EI_{crack}=MN/\varphi_y$ and rotational hinges at the ends and at mid span. The moment-rotation capacity of the hinges was obtained from the moment-curvature sectional analysis with assumptions for the plastic hinge length L_p and strain penetration length L_{sp} according to Priestley et al. (2007). The moment-curvature was obtained assuming confined compression strength of the concrete core according to Mander et al. (1988) and axial force in the elements from static analysis with soil pressure at rest.

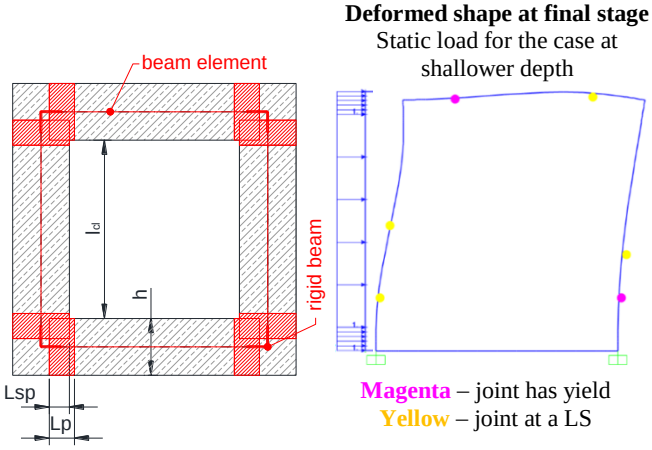

Figure 4 Example of the global failure mode considered for the estimation of the capacity of the structure and geometry of the FE model used for that

Three different damage limit states were considered according to the material strain limits by Priestley et al. (2007), together with premature brittle shear failure of a section, which was assumed to cause a global structural instability and ULS. The damage states are: Serviceability Limit State (SLS), when spalling of the concrete cover initiates, cracks have appeared with a residual width around 1mm and repair should not be needed; Damage Limit State (DLS), when crushing of the concrete core has occurred, the transverse reinforcement might have ruptured and the structure needs substantial repair; Ultimate Limit State (ULS), when the joints have reached their ultimate capacity and the structure is near collapse and cannot be repaired.

The shear capacity was evaluated in two ways. The first one was by following procedures and recommendations by Priestley et al. (1996,2007), Kowalsky and Priestley (2000) and Montejo and Kowalsky (2007). According to them the capacity consists of three components: steel truss mechanism, concrete shear strength and axial load contribution on an element level. This capacity was then compared to the shear demand on the element from its full flexural capacity. The second one was by accounting for the moment-shear-axial (M-V-N) load interaction on a sectional level. This relationship was obtained by applying the Modified Compression Field Theory (MCFT) by Collins (1997), implemented in a routine by Bentz (2000). When the M-N and M-V interaction diagrams are combined, they form a M-V-N capacity surface (Figure 7). All things considered, the global capacity of the structure for two depths are presented in Figure 5.

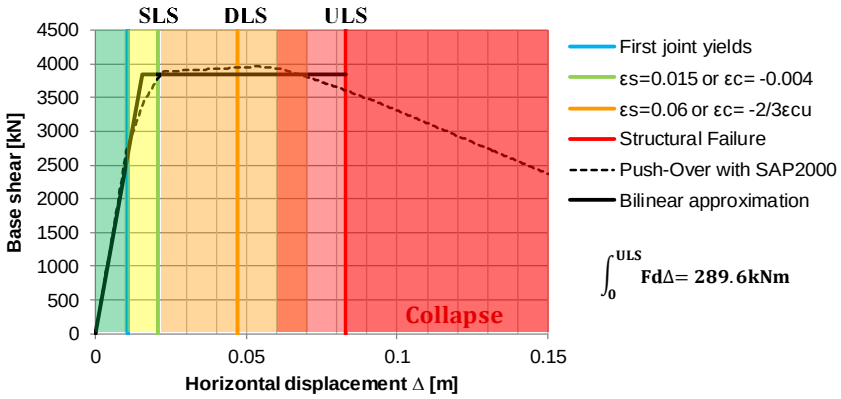

Figure 5 Push-Over curves from SAP2000, their bilinear approximation and damage limit states for structure at shallow depth d_t

CAPACITY VS. DEMAND

The response of the structure to the induced vibrations and the expected damage was evaluated in several ways, grouped in two categories: 1) without direct consideration for structural capacity, which included implementation of seismic intensity scales (Comission European Seismological, 1998; USGS, http://earthquake.usgs.gov) and adopting intensity prediction equations (Atkinson and Kaka, 2006; Sorensen, et al., 2008) in function of PPV, comparison of the PPA to the site hazard and comparison of PPV to published damage limits for buried facilities (Lucca, 2003); 2) with direct consideration for the structural capacity, which included comparison of the induced drift to the structural drifts at certain damage states, comparison of the force demand to the structural capacity and implementation of pressure (force) - impulse diagrams.

Pressure – impulse diagrams are curves, which allow easier assessment of structural response to a specific load (Figure 6). The asymptotes refer to two load regimes: 1) quasi-static, when the natural period of the structure is much shorter than the load duration and the load may be considered to remain constant while the structure attains its maximum deflection; 2) impulsive, when the load duration is much shorter than the natural response period and the load has finished acting before the structure has had time to respond significantly. If the load duration and the natural period are comparable, the load regime is called dynamic and it requires detailed dynamic analysis. Once the displacement limits of the structure at different damage states are known, the pressure impulse curves indicate the combination of load and impulse that will cause

a certain level of damage. The structure is damaged, only if it falls to the right and above the curves for a certain damage state. The location of the asymptotes is obtained by equating the work done by the induced pressure to the strain energy and the kinetic energy to the strain energy. (Figure 6).

Examples for the evaluation of the damage potential are shown in Figure 7 for premature local failure of a section and in Figure 8 for global structural failure with demand for Method 1. The results from Method 2 and Method 3 were interpreted in a similar way.

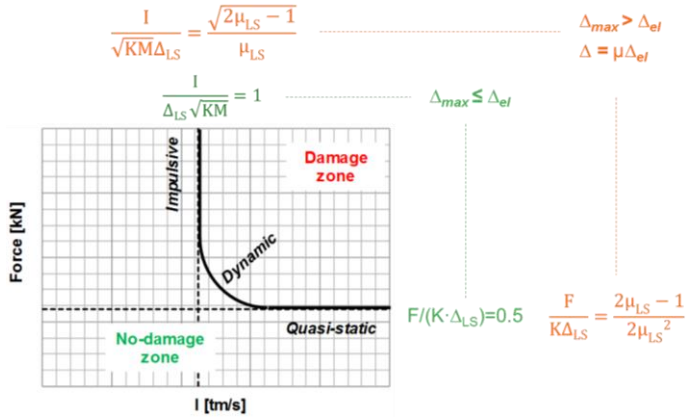

Figure 6 Pressure-Impulse diagrams. The asymptotes in green refer to an elastic single-degree of freedom system and does in orange to an elastic-perfectly plastic one

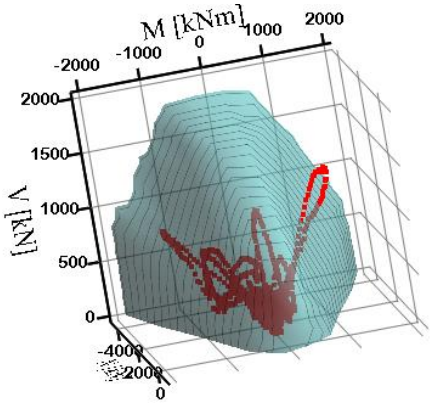

Figure 7 Results from Method 4. Large Commercial Aircraft. Structure at depth $2.3d_t$ and distance $1.5l_i$, vertical element

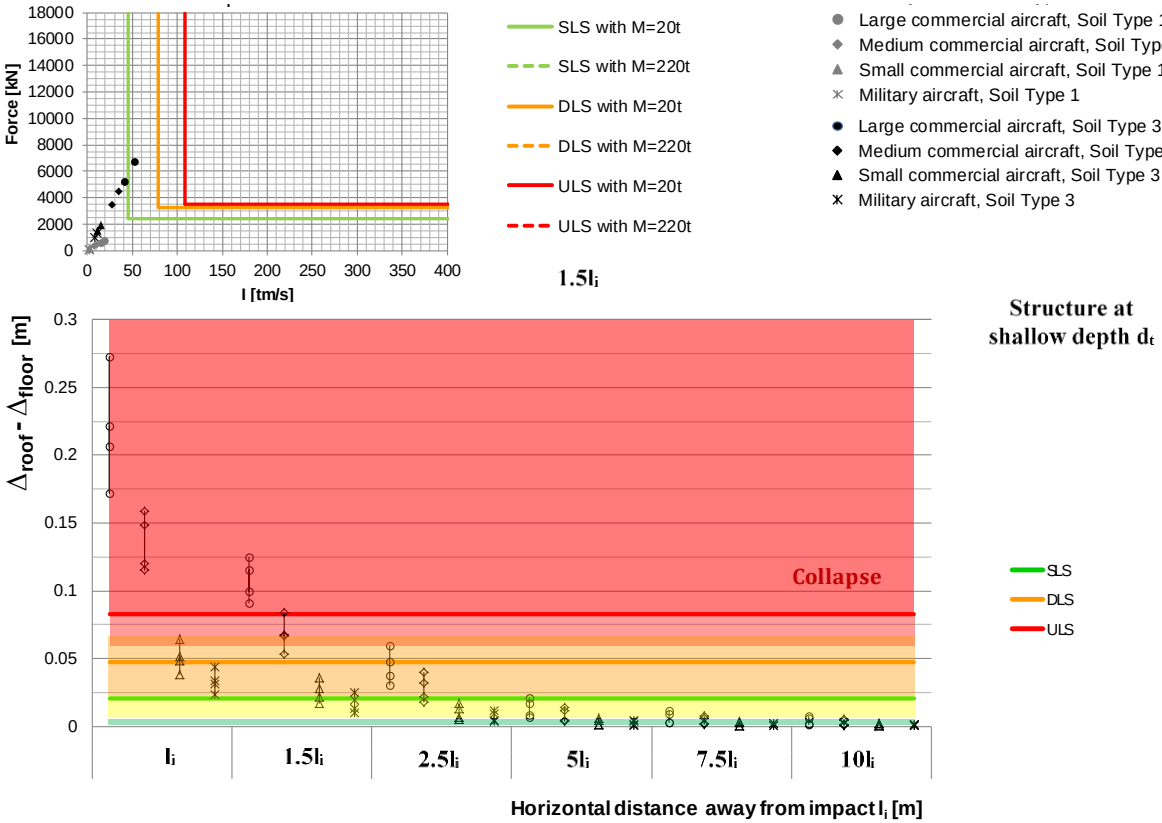

Figure 8 Some results with the demand obtained from analysis Method 1

The following observations from the comparison of the results from the four methods are worth noting: • Method 1 is much less sensitive to the type of soil than Method 2, for which the difference in the

attenuation of the induced vibration between the two soil types is substantial; • The attenuation of the vibration with distance for Method 2 is much steeper compared to the other two analysis methods; • In general, Method 2 led to highest intensities (PPV, PPD and PPA) and Method 3 to the lowest; Greater dispersion of the results among the types of aircraft was observed for Method 2 compared to the other methods; • For Method 1 the intensity of the induced vibration is proportional to the mass and velocity of the aircraft, so the heavier and faster the aircraft, the larger the intensity. This is not the case for the other two methods, where the area of the impact footprint also plays a role and the Small Commercial and Military aircraft are predicted to cause greater damage in proportion to the damage by Large and Medium Commercial aircraft; • Method 3 best captures the types of propagating waves and the energy transmitted with them, whereas for the other two methods the type of the wave that could cause the substantial damage is assumed at the start; • Method 4 directly considers the soil-structure interaction and was successfully used to refine the damage-potential analysis at close distances to the impact zone for more accurate predictions.

DAMAGE POTENTIAL – DISTANCE / DAMAGE MATRICES

The objective of the study is to investigate the damage potential of different aircraft impacts to a buried RC structure by implementing different methods for the analysis of the demand and different ways to quantify the response of the structure to the load. Each method is based on a theory that deviates from the real physics of the problem, has strong and weak aspects, and is loaded with uncertainties. In order to assess the influence of these uncertainties on the final results, a "confidence tree", which weigh the level of confidence of the results from each method was used, analogous to the logic-tree methodology. The confidence levels were assigned based on engineering judgement and experience. These levels can be very easily altered, in case additional information calls for it. Figure 9 shows the concept of the confidence tree and how the final distance-damage matrices were obtained based on it.

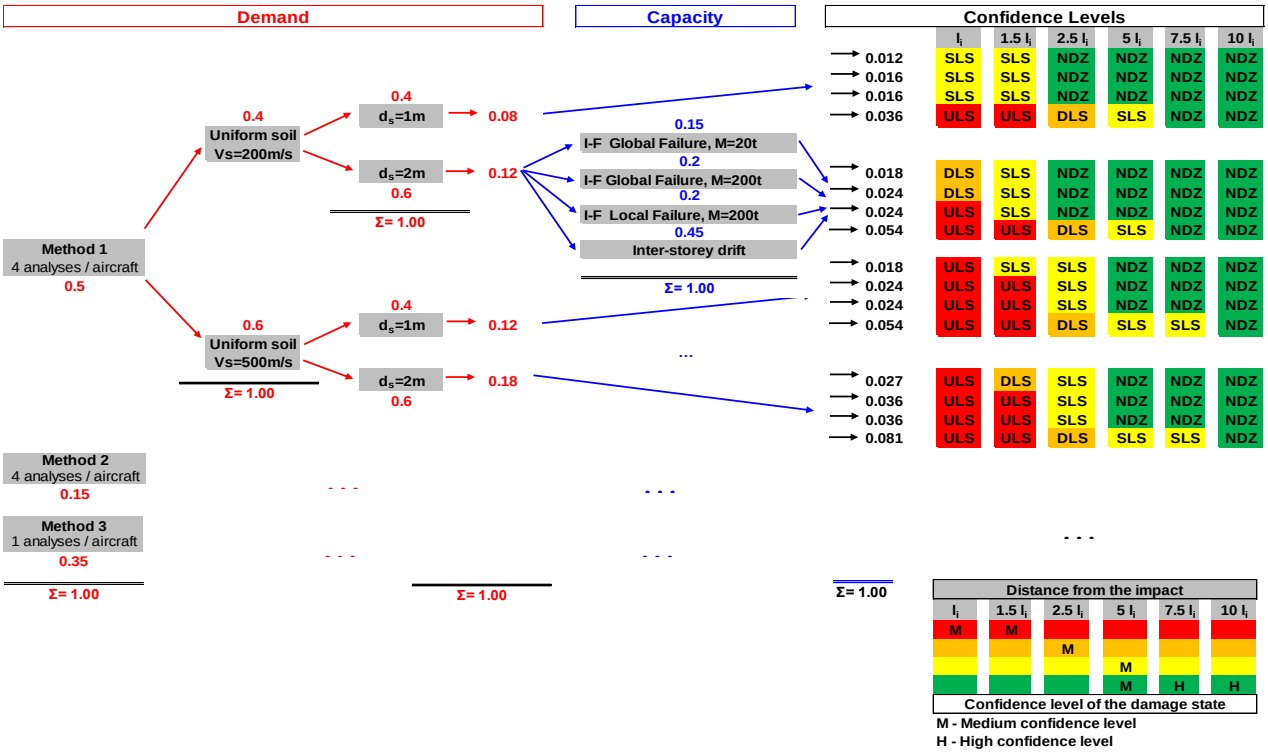

Figure 9 Methodology of the confidence-level tree. The final distance-damage matrix (bottom-right) corresponds to the case with structure at shallower depth and load with large commercial aircraft

The confidence levels are indicated with the red figures for the methods used for the evaluation of the demand, blue figures for the methods used to correlate capacity with demand and the black figures show the final confidence levels obtained by multiplying the numbers from the previous branches. With this numbers in black, each damage level was weighed and then summed up among all methods to give the final confidence matrices of damage states for each aircraft at six different locations away from the impact zone and two different depths. For clarity the results were simplified to two confidence levels: Medium (M) for a sum between 33% and 66% and High (H) for a sum ≥ 66% .

By applying this confidence tree for the considered depths and the four types of aircraft, distance-damage matrices were obtained for all cases. This helped to predict zones at which severe damage to collapse and no- to slight damage to the structure could be easily filtered out and for the other damage states the zones could be distinguished with certain level of confidence.

CONCLUSIONS

This paper describes a study on the evaluation of the severity of the damage to an underground RC structure due to a possible AI on the site platform. Different methods for the evaluation of the intensity of the induced vibrations and the capacity of the structure were implemented. Their strong and weak aspects were discussed and the results were compared. Since the analytical methods are a simplification of the physical phenomena, the results from them vary and are loaded with uncertainties. That is why, the conclusions were presented in terms of damage-distance matrices, for which the damage states are predicted with certain level of confidence based on a "confidence tree", analogous to the logic tree method. With these matrices, zones with certain structural failure and no-damage zones could be easily predicted.

The substantial variation in the outcome among the methods is explained with the high sensitivity of the results to the assumptions and the initial parameters. This study presents an example of how the results from a certain theory should be interpreted with caution and should be compared to other theories or experimental results, when available, especially for complicated problems like aircraft impact. The "confidence tree" presented in this paper is an easy-to-implement tool to evaluate the uncertainties of the analysis and to present the results in a way that is easy to interpret in the context of a real project.

NOMENCLATURE

c – *seismic wave velocity*
d_s – *depth of impact*
d_t – *depth of the points of interest*

E_c – *elastic modulus of concrete*
f_c – *dimensionless coupling factor*
h – *width of the RC sections*
H – *thickness of the soil cover layer*
K – *stiffness*
l_{cl} – *clear span of the walls of the buried structure*
l_{col} – *length of equivalent soil column*
l_i – *horizontal distance from impact to a point*

β – *coefficient for the arching effect in*
γ – *specific weight of soil*
μ – *displacement ductility*

M – *moment*
M_{AIC} – *mass of aircraft*
M_N – *nominal moment at* φ_y ε_c*=-0.004 or* ε_s*=0.015*
M'_y – *moment at first yield of a rebar*
n – *attenuation coefficient*
N – *axial load*
R – *shortest distance from impact to a point*
t_d – *impact duration*
V – *shear force*
V_0 – *initial velocity*
Vs – *shear wave velocity*

ρ – *density of the soil*
φ_y – *nominal curvature* $\varphi_y=\varphi'_y \cdot M_N/M'_y$
φ'_y – *curvature at first yield of the reinforcement*

REFERENCES

Amick, H., & Gendreau, M. (2000). Construction vibrations and their impact on vibration-sensitive facilities. *ASCE Construction Congress 6.* Orlando, Florida.

Atkinson, G., & Kaka, S. (2006). Relationships between Felt Intensity and Instrumental Ground Motion for New Madrid ShakeMaps. *Dept. of Earth Sciences, Carleton University*.

Bentz, E. (2000). *Sectional analysis of reinforced concrete.* PhD Thesis, University of Toronto, Department of Civil Engineering.

CEN European Committee for Standardization. (2004). *Eurocode 7: Geotechnical design - Part 1: General rules.*

Collins, M., & Mitchell, D. (1997). *Prestressed concrete structures.* Response Publications, Canada.

Comission European Seismological. (1998). *European Macroseismic Scale.* (G. Grünthal, Ed.) Luxembourg.

Dowding, C. (2000). *Construction vibrations. Second edition.* Upper Saddle River, NJ: Prentice Hall Engineering/Science/Mathematic.

Geotechnical Engineers Inc. (GEI). (1983). *Evaluation of Dynamic Soil Profiles for the F-Area Sand Filter Structures.* Boston, MA.

HA SEDD NAWCCC DRD. (2001). *Design Manual for Roads and Bridges. Volume 2: Highway Strucure Design (Substructures, Special structures and materials). Section 2: Special Structures. Part 12. BD 31/01. The design of buried concrete box and portal frame structures.*

Headquarters Department of the Army. (1986). *Fundamentals of protective design for conventional weapons.* Technical Manual 5-855-1, Washington, D.C.

Idriss, I., & Sun, J. (1992). *SHAKE91: a computer program for conducting equivalent linear seismic response analyses of horizontally layered soil deposits.* Davis, California: Center for Geotechnical Modelling, Department of Civil and Environmentall Engineering, University of California.

Kokusho, T., & Esashi, Y. (1981). Cyclic triaxial test on sands and coarse materials. *Proceedings of the 10th international conference on soil mechanics and foundation engineering , 1*, pp. 673-676. Stockholm.

Kowalsky, M., & Priestley, M. (2000). Improved analytical model for shear strength of circular reinforced concrete columns in seismic regions. *ACI Structural Journal , 97*(3).

LSTC. (2014). *LS-DYNA. Keyword user's manual. Volume II. Material models.*

LSTC. (n.d.). *Livermore Software Technology Corporation*. Retrieved from http://www.lstc.com

LSTC. (n.d.). *LS-DYNA.* Retrieved from http://www.lstc.com/products/ls-dyna

Lucca, F. (2003). *Tight construction blasting: ground vibration basics, monitoring and prediction.* Terra Dinamica L.L.C. - effective blast design and optimization.

Mander, J., Priestley, M., & Park, R. (1988). Theoretical stress-strain model for confined concrete. *J. Struct. Engin., ASCE, 8*(114), 1804-26.

Montejo, L., & Kowalsky, M. (2007). *CUMBIA. Set of codes for the analysis of reinforced concrete members.* Technical Report No. IS-07-01, NC State University, Construction Facility Laboratory. Department of Civil, Construction and Environmental Engineering.

Priestley, M., Calvi, G., & MJ, K. (2007). *Displacement-based seismic design of structures.* Pavia, Italy: IUSS Press.

Priestley, M., Seible, F., & Calvi, G. (1996). *Seismic Design and Retrofit of Bridge Structures.* New York: John Wiley and Sons.

Smith, P., & Hetherington, J. (1994). *Blast and Balistic Loading of Structures.* Oxford, Great Britain: Butterworth-Heineman Ltd.

Sorensen, M., Stromeyer, D., & Grünthal, G. (2008). Estimation of macroseismic intensity - new attenuation and intensity vs. ground motion relations for different parts of Europe. *The 14th World Conference on Earthquake Engineering.* October 12-17, Beijing, China.

USGS. (n.d.). *USGS*. Retrieved from Earthquake Hazards Program: http://earthquake.usgs.gov/learn/topics/mercalli.php

Zen, K., Umehara, Y., & Hamada, K. (1987). Laboratory tests and in situ seismic survey on vibratory shear modulus of clayey soils with various plasticities. *Proc., 5th Japanese Earthquake Engineering*, (pp. 721-728). Japan.